Decrypting geophysical signals at Stromboli Volcano (Italy): Integration of seismic and Ground-Based InSAR displacement data

AGU PUBLICATIONS

Geophysical Research Letters

RESEARCH LETTER
10.1002/2014GL059824

Key Points:
- Integration of seismic and Ground-Based InSAR displacement data at Stromboli
- Correlation between inflation, volcanic tremor, and rate of VLP events
- Passive gas transfer in the conduit is delayed with respect to slug formation

Correspondence to:
F. Di Traglia,
ditragliafederico@gmail.com;
federico.ditraglia@unifi.it

Citation:
Di Traglia, F., L. Cauchie, N. Casagli, and G. Saccorotti (2014), Decrypting geophysical signals at Stromboli Volcano (Italy): Integration of seismic and Ground-Based InSAR displacement data, *Geophys. Res. Lett.*, *41*, 2753–2761, doi:10.1002/2014GL059824.

Received 5 MAR 2014
Accepted 27 MAR 2014
Accepted article online 31 MAR 2014
Published online 16 APR 2014

Decrypting geophysical signals at Stromboli Volcano (Italy): Integration of seismic and Ground-Based InSAR displacement data

F. Di Traglia[1,2], L. Cauchie[3,4], N. Casagli[1], and G. Saccorotti[3]

[1]Department of Earth Sciences, Università degli Studi di Firenze, Firenze, Italy, [2]Department of Earth Sciences, Università degli Studi di Pisa, Pisa, Italy, [3]Sezione di Pisa, Istituto Nazionale di Geofisica e Vulcanologia, Pisa, Italy, [4]School of Geological Sciences, University College of Dublin, Dublin, Ireland

Abstract We present the integration of seismic and Ground-Based Interferometric Synthetic Aperture Radar system (GBInSAR) displacement data at Stromboli Volcano. Ground deformation in the area of summit vents is positively correlated with both seismic tremor amplitude and cumulative amplitudes of very long period (VLP) signals associated with Strombolian explosions. Changes in VLP amplitudes precede by a few days the variations in ground deformation and seismic tremor. We propose a model where the arrival of fresh, gas-rich magma from depth enhances gas slug formation, promoting convection and gas transfer throughout the conduit system. At the shallowest portion of the conduit, an increase in volatile content causes a density decrease, expansion of the magmatic column and augmented degassing activity, which respectively induce inflation of the conduit, and increased tremor amplitudes. The temporal delay between increase of VLP and tremor amplitudes/conduit inflation can be interpreted in terms of the different timescales characterizing bulk gas transfer versus slug formation and ascent.

1. Introduction and Rationale for the Study

Located in the Tyrrhenian Sea off the southern coast of Italy, Stromboli Volcano (Figure 1) gives the name to Strombolian activity, characterized by mild, intermittent explosions occurring at a typical rate of 1–10 events per hour [*Blackburn et al.*, 1976]. Individual explosions are driven by large gas slugs that, upon reaching the surface of the magma column, cause the sudden release of gas accompanied by the ejection of molten lava fragments [*Blackburn et al.*, 1976]. This activity usually involves degassed, high-porphyritic (HP) basaltic magma residing in the shallowest, cooled portion of the conduit system [*Bertagnini et al.*, 2003]. The ordinary Strombolian activity is occasionally interrupted by the occurrence of higher-intensity explosions, usually referred to as "major" or "paroxysmal" events [*Barberi et al.*, 1993]. These latter explosions are associated with the emission of deep-derived, volatile-rich, low-porphyritic (LP) basalt, often mingled with the HP basalt [*Rosi et al.*, 2013].

Stromboli is an open-conduit volcano and does not experience pressurization of the magma storage and/or plumbing system that produces ground deformations at the scale of the volcanic edifice. For any such system, localized inflation or deflation may occur in response to conduit processes, such as magma convection and uprising [e.g., *Chaussard et al.*, 2013]. Detectable ground deformation at Stromboli has only been observed in association with dyke intrusion at shallow depth, prior to the opening of new eruptive fractures [e.g., *Casagli et al.*, 2009; *Aloisi et al.*, 2008].

In this work we analyze weak deformations recorded by a Ground-Based Interferometric Synthetic Aperture Radar system (GBInSAR) [*Antonello et al.*, 2004] and ground displacements in the seismic band (0.02–10 Hz) at Stromboli Volcano, in order to improve our understanding of the geophysical signals associated with magma dynamics in an open volcanic system. We analyze the period spanning 6 June 2011 to 27 August 2011, which was characterized by activity of higher intensity than usually observed. This period was preceded by more than 2 months of increase in both CO_2 flux and displacement rate at the base of the NE vents area (up to 0.55 mm/h on 8–10 May 2011) [*Di Traglia et al.*, 2013]. The period under study also includes seven major explosions and two lava overflows from the NE vents (1–2 August and 18 August 2011) [*Nolesini et al.*, 2013].

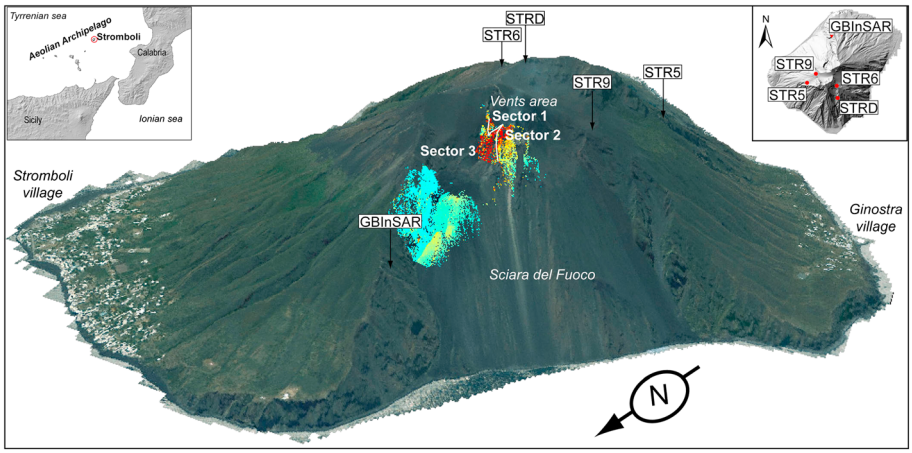

Figure 1. Perspective view of Stromboli Volcano from the northwest. Locations of the seismic stations used for this study are indicated by arrows and labeled STR5, STR6, STR9, and STRD. Colored areas span the GBInSAR field of view; colors correspond to the total displacement cumulated during the period under study (June 2011 to August 2011; see Figure 2a for the color scale). The inset at the top left indicates the position of Stromboli with respect to Southern Italy; the inset at the top right shows the instrument location in map view.

2. Instruments

2.1. The GBInSAR Monitoring System

Since 2003, the northeast portion of the summit vents area of Stromboli Volcano (Figure 1) has been continuously monitored by a GBInSAR system, consisting of a transmitting and a receiving antenna moving along a 3 m long rail [*Antonello et al*., 2004]. The GBInSAR measures ground displacement along the line of sight (LOS; Figure 1), by computing via cross correlation, the phase differences between the backscattered signals associated with two consecutive synthetic aperture radar (SAR) images. The ability of InSAR analysis to measure volcano deformation depends on the persistence of phase coherence over appropriate time intervals. The loss in coherence is primarily due to messy ground movements, e.g., grain avalanches [*Antonello et al*., 2004]. A coherence threshold set to 0.8 is therefore adopted to reject the noisy areas of the interferogram [*Di Traglia et al*., 2014]. Due to the short lapse time (11 min) between two subsequent measurements, the interferometric displacements are usually smaller than half wavelength, and phase-unwrapping procedures [*Ghiglia and Romero*, 1994] are not necessary. Both the range and cross-range resolutions are on average 2 m × 2 m, with a precision in displacement measurements of less than 1 mm [*Casagli et al*., 2009]. The precision in the displacement measurement is 0.1 mm for punctual (few pixels) automatic extraction or 0.5 mm for data associated with homogeneous sector, when the selection is performed manually based on visual inspection [*Di Traglia et al*., 2014]. Displacement rates are obtained through the time differentiation of displacements obtained from two consecutive images.

2.2. The Seismic Monitoring Network

Seismic data used in this work are from four stations belonging to the permanent, broadband seismic network monitoring Stromboli Volcano since 2003. The network is composed of 13 instruments distributed at different elevations and back azimuths with respect to the summit craters. The seismic sensors are Guralp CMG-40T with flat response over the 0.016–50 Hz frequency range, whose signals are digitized locally at a rate of 50 samples/s with a resolution of 24 bits, and then radio transmitted to an acquisition center located on the island. The location of the seismic stations used for this study is shown in Figure 1. Before analysis, seismic data are corrected for instrument response and converted to displacement.

3. Data

3.1. Cumulative Displacement Maps and Displacement Time Series

The analysis of displacement is performed only on the flanks of the vents area (Figure 2a) [*Di Traglia et al*., 2014, sector 2]. The GBInSAR is located in a stable area, and its LOS is mostly sensitive to the N-S components of displacement (Figure 2a). Negative and positive values of displacement indicate, respectively, a movement

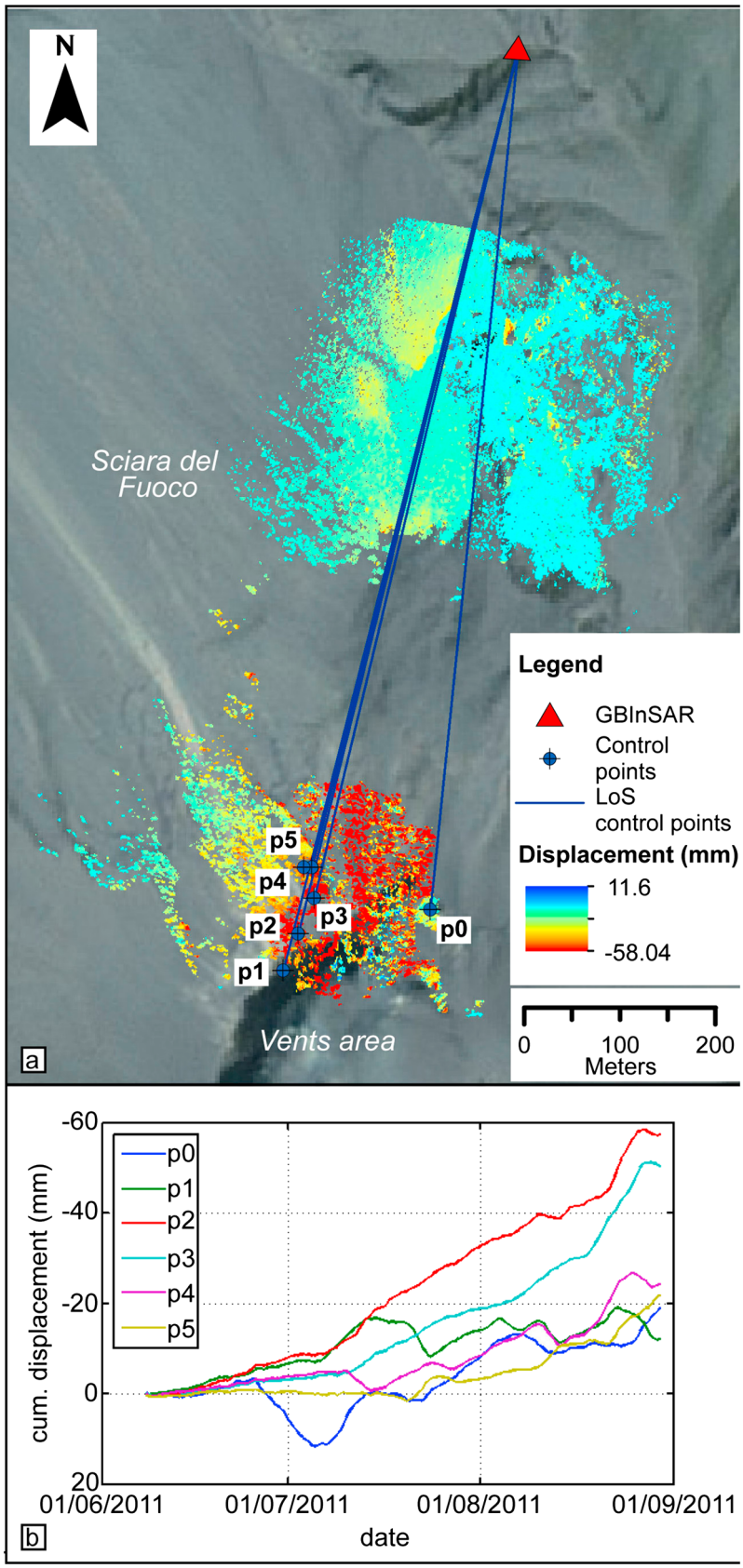

Figure 2

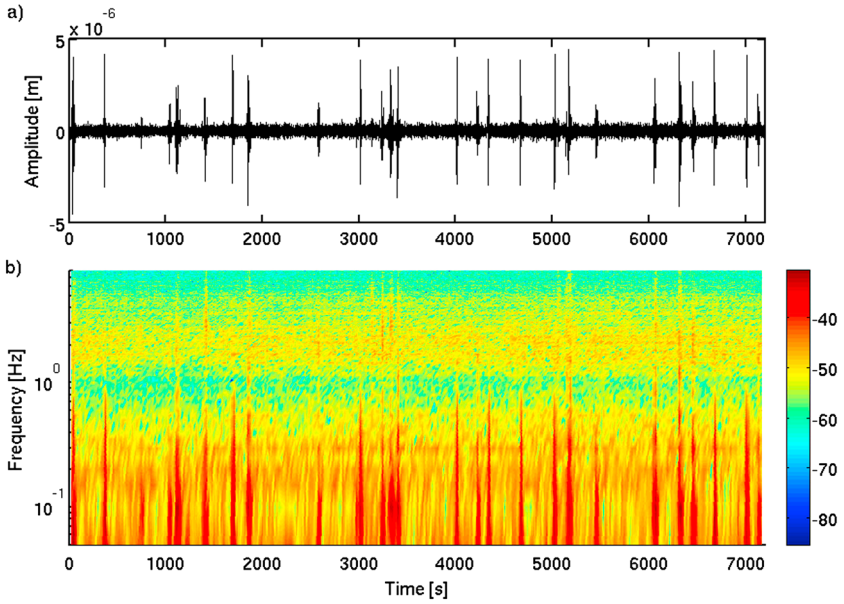

Figure 3. (a) Two hour long seismogram from the vertical component of station STR9. The associated spectrogram (b) highlights stationary signals over the 1–4 Hz and 0.1–0.4 Hz frequency bands. VLP pulses are peaked between 0.05 and 0.5 Hz.

toward and away from the sensor (i.e., inflation and deflation, respectively, of the summit vents area). Cumulative GBInSAR displacement maps for specific time intervals are obtained by summing, pixel by pixel, the differential displacements recorded by 12 h interferograms [*Intrieri et al.*, 2013].

Displacement time series of selected points (~10 pixels) were obtained from the cumulative displacement maps. Five points (P1 to P5; Figure 2a) were selected in sector 2, and a reference point (P0) was selected in a zone of the vents area that shows little displacement. The selected points show different displacement trends. In particular, points P2 through P5 show similar trends, with inflation since late June until late August, while P1 exhibits a slightly different behavior (Figure 2b). The difference in the displacement trend of P1 can be explained as the results of an artifact due to its position with respect to the GBInSAR's LOS. P1 is located on the external rim of the vents area, and its displacement vector is thus expected to be directed mainly along the NW-SE direction, with negligible components along the LOS (NS) direction. P2 to P5 are located in the northern part of the vents area, and their displacement vectors are mainly oriented NS [*Di Traglia et al.*, 2014]. Differences in displacement trends between points P2–P3 and P4–P5 are related to the geometry of the displacement in the vents area, as evidenced in the cumulative maps. In fact, P2–P3 are located in the upper part of the vents area that is characterized by the maximum displacements, while P4–P5 are located at a lower elevation, near the limit between sector 2 and sector 3, where only small displacements have been observed.

The geometry of the displacement indicates that the dislocation decreases downslope, in agreement with an inflation of the summit vents area. The trend of differential GBInSAR displacement (Figure 4a) shows three periods of inflations and deflations. Inflation was recorded between 7 and 13 July 2011, followed by a deflation until 17 July 2011, when a major explosion occurred (Figure 4a). Inflations also occurred between 3 and 8 August 2011, followed by a deflation until 10 August, and between 18 and 23 August 2011, followed by a deflation until 28 August (Figure 4a). In both latter cases, the inflations followed the occurrence of lava overflows (on 1 and 18 August 2011, respectively).

3.2. Seismic Data

Figure 3 illustrates the time-frequency transform (spectrogram) for a 2 h long recording from the vertical component of station STR9. Sustained signals spanning the 1–4 Hz and 0.1–0.4 Hz frequency bands are

Figure 2. (a) Map view of the GBInSAR cumulative displacement map for the June 2011 to August 2011 time interval. The control points P0–P5 are indicated by blue circles; the GBInSAR location is marked by a red triangle. Line-of-sight path to the control points are marked by blue lines. (b) Cumulative time series of GBInSAR-displacements at the reference points.

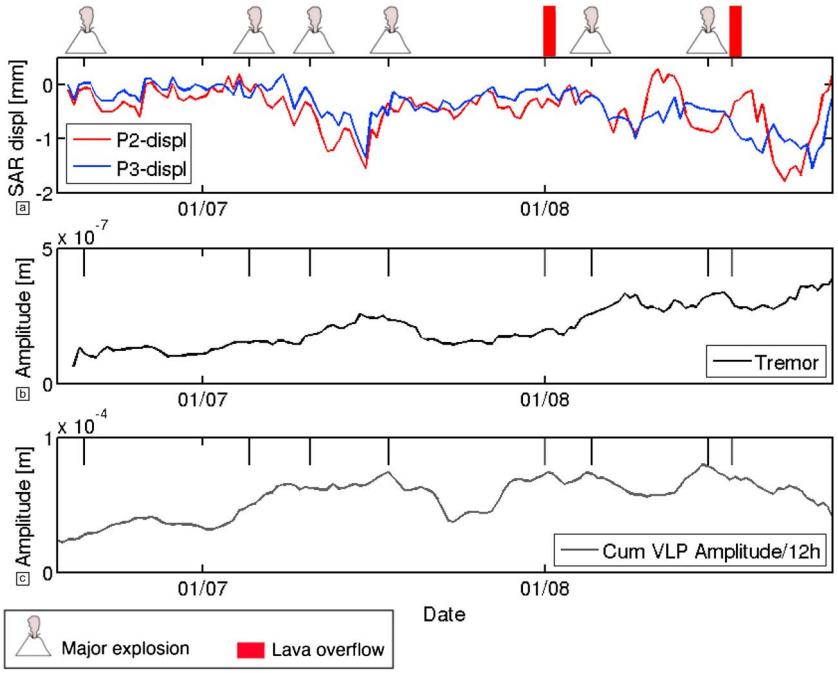

Figure 4. (a) Time series of GBInSAR differential displacements at reference points P2 and P3 (red and blue, respectively). (b) Tremor amplitude. (c) VLP amplitudes cumulated over 12 h long, nonoverlapping time windows. The analyzed time interval spans from 6 June through 27 August 2011.

associated with volcanic tremor [e.g., *Chouet et al*., 1997] and oceanic microseisms [*Braun et al*., 1996], respectively. Using the same station and component, we estimated tremor intensity throughout the analyzed time interval by computing the RMS amplitudes of 1–3.5 Hz band-pass-filtered seismograms over nonoverlapping, 12 h long time windows (Figure 4b).

Very long period (VLP) signals associated with the summit explosions [e.g., *Chouet et al*., 2003] are superimposed on the tremor and microseism activity. During the period of analysis, VLPs occurred at a rate of about 5–10 events per hour. They are characterized by a typical duration of about 40 s and a low-frequency content, with most of the energy concentrated within the 0.05–0.5 Hz frequency band (Figure 3b). Over the period of this study, we detected 9183 events by using a short-time-average through long-time-average (STA/LTA) approach [*Earle and Shearer*, 1994]. Data were filtered in the 0.05–0.5 Hz frequency band; windows of 4 and 60 s were used for computing the short- and long-term averages, respectively. An event is declared whenever at least three stations exhibit an STA/LTA ratio greater than 3.5. A final verification of the consistency of the VLP catalog is performed by calculating the polarization attributes using the eigen decomposition of the covariance matrix of the three components of ground motion [*Kanasewich*, 1981]. At station STR9, results associated with the first pulse of VLP signals give azimuthal polarization angles centered around 152°, which is consistent with a source located beneath the central and NE vents.

VLP signals are thought to represent the elastic response of the shallow conduit system to pressure instabilities associated with the transit of large gas slugs driving Strombolian explosions; VLP amplitudes, which are linearly related to the volumetric deformation at the source, can therefore be taken as a proxy for the amount of volatiles involved into the explosive process [*Chouet et al*., 2003]. For a direct comparison with SAR and tremor time series, maximum peak-to-peak amplitudes of individual VLP events at station STR9 are cumulated over subsequent, 12 h long time windows (Figure 4c).

Both the tremor and cumulative amplitudes of the VLP events exhibit fluctuations at periods on the order of several weeks, superimposed on a general increase that lasts throughout the whole observation period. This positive trend correlates well with the overall inflation observed in Figure 2b; however, since these latter changes occur over a timescale which is longer than the duration of our observations, they will not be discussed any further throughout the rest of this paper.

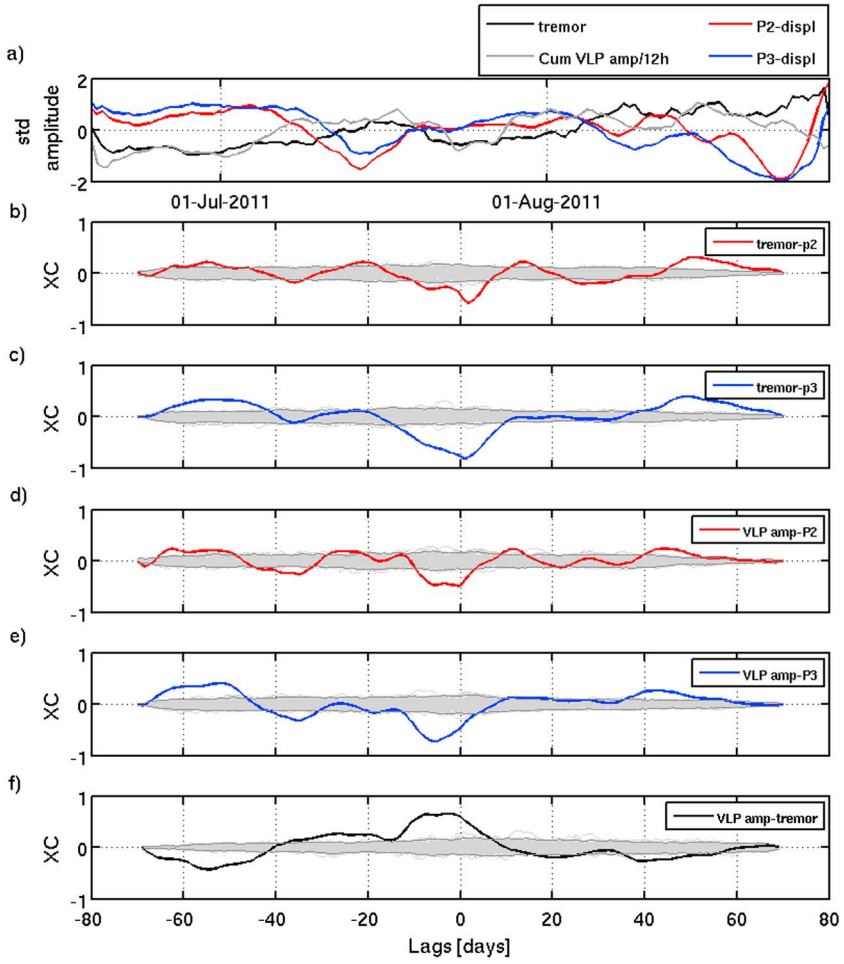

Figure 5. Results from correlation analysis. (a) Standardized time series of GBInSAR differential displacements, tremor and VLP amplitudes. (b–e) Cross-correlation functions between the GBInSAR displacements at control points P2–P3 and tremor/VLP amplitudes. (f) Cross correlation between VLP and tremor amplitudes. In all the panels, gray bands indicate the CCFs obtained after randomization of the time series; dark gray lines are the 95% confidence level on correlation estimates.

4. Correlations

Figure 4 shows the time histories of GBInSAR differential displacements at control points P2–P3, tremor, and VLP amplitudes, with the most relevant effusive and explosive episodes occurring during the analyzed time interval, indicated above the figure. Simple visual inspection indicates an anticorrelation between the deformation and tremor amplitude time series, where inflation/deflation are respectively accompanied by an increase (8–16 July 2011; 31 July to 8 August 2011; and 18–24 August) and a decrease (17–26 July; 8–12 August 2011; and 17–24 August) of tremor activity. In order to quantitatively assess the relationships between these time series, we proceed with an evaluation of the cross-correlation function (CCF) among the seismic and GBInSAR recordings. Before the analyses, the different time series are first standardized (i.e., demeaned and divided by their standard deviation), and then smoothed using a 5 day long moving window. Results confirm the negative correlation between tremor and deformations (Figures 5b and 5c). For both P2 and P3 control points, the highest, absolute-value correlations (equal to -0.6 and -0.8, respectively) are observed at a time lag of 1 day. This lag time implies an almost simultaneous occurrence of the inflation in the vents area and the increase in tremor amplitude.

Correlation functions between GBInSAR displacements, tremor amplitudes, and cumulated VLP displacements exhibit broad absolute-value maxima which, for all the instances, span negative lag times in between 2 and 6 days (Figures 5d and 5e). This implies that the variations in the cumulative volume change associated with summit explosions precede both the deformation of the vents area and the associated

changes of tremor amplitudes. The statistical significance of the retrieved CCFs is tested using the method proposed by *Martini et al.* [2009]. The computation of the different CCFs is repeated for 100 runs, each time randomizing one of the two time series. The set of correlation coefficients thus obtained are then transformed to a normally distributed variable using Fisher's *z*-transform [*Saccorotti and Del Pezzo*, 2000], allowing for derivation of the mean (ccm) and standard deviations (ccs) of the correlation coefficients at each time lag. At any given time lag, the CCF between the two analyzed variables is considered significant at the 95% confidence level if the module of the associated correlation estimate is greater than the threshold (ccm ± 2*ccs) obtained from the randomization test. In Figures 5b–5f, the set of the CCFs computed from the permuted time series and the corresponding 95% significance level are shown in light and dark gray, respectively.

5. Discussion and Concluding Remarks

In the previous sections we showed that the wide-band (periods spanning the 10^0 s to10^5 s range) ground displacements at Stromboli Volcano exhibit significant correlations at different time lags. In particular, the GBInSAR system reports inflation and deflation of the vents area (Figure 1, sector 2) that are (i) coupled to changes in the tremor amplitude and (ii) preceded by variations in the cumulative amplitude of the VLP signals. Numerical modeling of the geomechanical behavior of Stromboli suggests that changes in the magmastatic pressure accompanying variations in magma level are sufficient to produce measurable displacements of the external flank of the vents area [*Casagli et al.*, 2009]. Volcanic tremor at Stromboli Volcano is primarily associated with the phenomena of steady quiescent degassing. In particular, it has been related to the intermittent bursting of small ($<$ 1 m) bubbles at the free surface of the magma column (*gas puffing*) [*Ripepe and Gordeev*, 1999], as also indicated by the shallowness of the tremor source [e.g., *Saccorotti et al.*, 1998]. The coupling between the deformation of the summit vents area with tremor amplitude suggests that the variation in the magma level is related to increasing magma vesiculation, which implies enhanced degassing activity [see also *Colò et al.*, 2010].

More puzzling is the interpretation of the negative lag time exhibited by the VLP time series with respect to both the ground deformation and tremor amplitude temporal histories. The increase in the overall volume change associated with VLP signals before inflation implies that the slug formation and release precede the shallow magma vesiculation. Although this may appear as a paradox, it can be explained by the different processes which control gas transfer throughout the Stromboli conduit system, namely, slug formation and ascent versus steady state bulk transfer of volatiles.

Clues on the timescale of slug ascent are derived from geochemical evidence [*Burton et al.*, 2007b], which indicates that the gas slugs driving Strombolian explosions rise separately from the magma from depths between ~2.7 and 0.8 km below the vents, corresponding to the volcano-crust interface and sea level, respectively. Though different models exist to explain slug genesis [e.g., *Parfitt*, 2004], the present experimental evidence does not provide any constraints for discriminating the actual mechanism acting at Stromboli. Nonetheless, both slug frequency and explosion intensity are primarily controlled by a minimum gas volume accumulation or critical gas pressure [*Del Bello et al.*, 2012; *Taddeucci et al.*, 2013] which, in turn, are related to inputs of fresh, gas-rich magma from below. The ascent of the large gas slugs driving the summit explosions is expected to be primarily controlled by buoyancy [*Del Bello et al.*, 2012] and further favored by percolation [*Burton et al.*, 2007b]. Theoretical considerations indicate that within a pressure range between 100 MPa and 50 MPa (~3.6 km and ~1.8 km depth, respectively) vesiculating magma ascending within the conduit becomes permeable to gas flow [*Burton et al.*, 2007b]. For these rising mechanisms, slug ascent velocities would be on the order of 2–30 m s^{-1} [*Harris and Ripepe*, 2007; *James et al.*, 2006, 2008], thus implying rise times spanning the 10^1–10^3 s range.

Changes in the volatile content of the shallowest portion of the magmatic column may result from two main classes of processes. The first is a convection mechanism, for which the volatile-rich, light magma entering into the system would substitute the overlaying and denser, volatile-depleted magma [*Parfitt*, 2004; *Lautze and Houghton*, 2005; *Burton et al.*, 2007a; *Longo et al.*, 2008; *Witham*, 2011]. For an interface between the resident (HP) and fresh (LP) magmas located at 2–3 km depth [*Aiuppa et al.*, 2010], an entire convection cycle would occur over timescales on the order of hours to days (average magma ascent rate = 0.22 m s^{-1}) [*Burton et al.*, 2007a], as also indicated by petrological constraints [*Bertagnini et al.*, 2003] and numerical simulations [*Longo et al.*, 2008]. The second process simply involves bubbles rising through magma; in this

case, rise speeds would be on the order of 10^{-3} to 10° times the bubble diameter which, for centimeter-size bubbles, would imply rise times on the order of months/years (bubble ascent rate 10^{-5} to 10^{-6} m s^{-1}) [*Burton et al*., 2007a]. At present, we are not able to discern which of these two end-member processes contribute more to the steady state gas transfer throughout the plumbing system. It is certain, however, that both mechanisms develop over timescales which are significantly longer than those associated with the ascent of a deeply formed gas slug, thus providing a possible interpretation for the observed delay between explosion rates and summit deformation.

In conclusion, our observations suggest that the bulk increase of vesiculation at the shallowest portions of the magmatic column is delayed with respect to the transfer of large gas slugs formed at depth. The time delay is likely determined by the different mechanisms (magma convection versus separated, two-phase flow) that control the two processes. Further conditioning factors are obviously represented by changes in bubble nucleation and growth rates that could be influenced by the delay in vesiculation of the LP magma [*Rivalta et al*., 2013], and/or changes in gas flux from depth [*Belien et al*., 2010]. A quantitative assessment of the role played by each of these factors in determining gas transfer at Stromboli Volcano would require the analysis of extended time series, and additional constraints offered by the geochemical tracking of both quiescent and explosive degassing. Nonetheless, our findings open a new perspective toward the use of multidisciplinary geophysical signals for the understanding of conduit processes and the establishment of a robust framework for the early warning of paroxysmal activity.

Acknowledgments

This work has been sponsored in part by the National Civil Protection Department (DPC) within the framework of the SAR.net2 and InGrID projects. The DPC is acknowledged for supporting the project and permitting this publication. The authors are grateful to Ellegi-Lisalab for technical support during the 2011 eruptive crisis. L.C. is supported by the European Union Seventh Framework Programme (FP7/2007-2013) project NEMOH, grant agreement 289976. F.D.T. is supported by a postdoc fellowship founded by the Regione Toscana (UNIPI-FSE) under the project RADSAFE (UNIPI-4) in the framework of the research agreement between DST-UNIPI, DST-UNIFI, and Ellegi s.r.l.-LiSALab. The authors are grateful to M. Iguchi and P. Dawson for precious reviews and A.V. Newman for the editorial management.

The Editor thanks Phillip Dawson and an anonymous reviewer for their assistance in evaluating this paper.

References

Aiuppa, A., A. Bertagnini, N. Métrich, R. Moretti, A. Di Muro, M. Liuzzo, and G. Tamburello (2010), A model of degassing for Stromboli Volcano, *Earth Planet. Sci. Lett.*, *295*(1), 195–204.

Aloisi, M., A. Bonforte, M. Mattia, and G. Puglisi (2008), Ground deformations related to the effusive eruptions of Stromboli: The 2002–2003 case, in *The Stromboli Volcano: An Integrated Study of the 2002–2003 Eruption*, *Geophys. Monogr. Ser.*, vol. 182, edited by S. Calvari et al., pp. 247–257, AGU, Washington, D. C.

Antonello, G., N. Casagli, P. Farina, D. Leva, G. Nico, A. J. Sieber, and D. Tarchi (2004), Ground-based SAR interferometry for monitoring mass movements, *Landslides*, *1*(1), 21–28.

Barberi, F., M. Rosi, and A. Sodi (1993), Volcanic hazard assessment at Stromboli based on review of historical data, *Acta Vulcanol.*, *3*, 173–187.

Belien, I. B., K. V. Cashman, and A. W. Rempel (2010), Gas accumulation in particle-rich suspensions and implications for bubble populations in crystal-rich magma, *Earth Planet. Sci. Lett.*, *297*(1), 133–140.

Bertagnini, A., N. Métrich, P. Landi, and M. Rosi (2003), Stromboli Volcano (Aeolian Archipelago, Italy): An open window on the deep-feeding system of a steady state basaltic volcano, *J. Geophys. Res.*, *108*(B7), 2336, doi:10.1029/2002JB002146.

Blackburn, E. A., L. Wilson, and R. J. Sparks (1976), Mechanisms and dynamics of Strombolian activity, *J. Geol. Soc.*, *132*(4), 429–440.

Braun, T., J. Neuberg, and M. Ripepe (1996), On the origin of the long-period tremor recorded at Stromboli Volcano (Italy), *Ann. Geophys.*, *39*, 311–326.

Burton, M. R., H. M. Mader, and M. Polacci (2007a), The role of gas percolation in quiescent degassing of persistently active basaltic volcanoes, *Earth Planet. Sci. Lett.*, *264*(1), 46–60.

Burton, M. R., P. Allard, F. Muré, and A. La Spina (2007b), Magmatic gas composition reveals the source depth of slug-driven Strombolian explosive activity, *Science*, *317*(5835), 227–230.

Casagli, N., A. Tibaldi, A. Merri, C. Del Ventisette, T. Apuani, L. Guerri, J. Fortuny-Guasch, and D. Tarchi (2009), Deformation of Stromboli Volcano (Italy) during the 2007 eruption revealed by radar interferometry, numerical modelling and structural geological field data, *J. Volcanol. Geotherm. Res.*, *182*(3), 182–200.

Chaussard, E., F. Amelung, and Y. Aoki (2013), Characterization of open and closed volcanic systems in Indonesia and Mexico using InSAR time series, *J. Geophys. Res. Solid Earth*, *118*, 3957–3969, doi:10.1002/jgrb.50288.

Chouet, B., G. Saccorotti, M. Martini, P. Dawson, G. De Luca, G. Milana, and R. Scarpa (1997), Source and path effects in the wave fields of tremor and explosions at Stromboli Volcano, Italy, *J. Geophys. Res.*, *102*(B7), 15,129–15,150, doi:10.1029/97JB00953.

Chouet, B., P. Dawson, T. Ohminato, M. Martini, G. Saccorotti, F. Giudicepietro, G. De Luca, G. Milana, and R. Scarpa (2003), Source mechanisms of explosions at Stromboli Volcano, Italy, determined from moment-tensor inversions of very-long-period data, *J. Geophys. Res.*, *108*(B1), 2019, doi:10.1029/2002JB001919.

Coló, L., M. Ripepe, D. R. Baker, and M. Polacci (2010), Magma vesiculation and infrasonic activity at Stromboli open conduit volcano, *Earth Planet. Sci. Lett.*, *292*(3), 274–280.

Del Bello, E., E. W. Llewellin, J. Taddeucci, P. Scarlato, and S. J. Lane (2012), An analytical model for gas overpressure in slug-driven explosions: Insights into Strombolian volcanic eruptions, *J. Geophys. Res.*, *117*, B02206, doi:10.1029/2011JB008747.

Di Traglia, F., C. Ventisette, M. Rosi, F. Mugnai, E. Intrieri, S. Moretti, and N. Casagli (2013), Ground-based InSAR reveals conduit pressurization pulses at Stromboli Volcano, *Terra Nova*, *25*(3), 192–198.

Di Traglia, F., et al. (2014), The Ground-Based InSAR monitoring system at Stromboli Volcano: Linking changes in displacement rate and intensity of persistent volcanic activity, *Bull. Volcanol.*, *76*(2), 1–18.

Earle, P. S., and P. M. Shearer (1994), Characterization of global seismograms using an automatic-picking algorithm, *Bull. Seismol. Soc. Am.*, *84*(2), 366–376.

Ghiglia, D. C., and L. A. Romero (1994), Robust two-dimensional weighted and unweighted phase unwrapping that uses fast transforms and iterative methods, *J. Opt. Soc. Am. A Opt. Image Sci.*, *11*(1), 107–117.

Harris, A., and M. Ripepe (2007), Synergy of multiple geophysical approaches to unravel explosive eruption conduit and source dynamics—A case study from Stromboli, *Chem. Erde*, *67*(1), 1–35.

Intrieri, E., F. Di Traglia, C. Del Ventisette, G. Gigli, F. Mugnai, G. Luzi, and N. Casagli (2013), Flank instability of Stromboli volcano (Aeolian Islands, Southern Italy): Integration of GB-InSAR and geomorphological observations, *Geomorphology*, *201*, 60–69.

James, M. R., S. J. Lane, and B. A. Chouet (2006), Gas slug ascent through changes in conduit diameter: Laboratory insights into a volcano-seismic source process in low-viscosity magmas, *J. Geophys. Res.*, *111*, B05201, doi:10.1029/2005JB003718.

James, M. R., S. J. Lane, and S. B. Corder (2008), Modelling the rapid near-surface expansion of gas slugs in low-viscosity magmas, *Geol. Soc. London Spec. Publ.*, *307*(1), 147–167.

Kanasewich, E. R. (1981), *Time Sequence Analysis in Geophysics*, pp. 1–532, Univ. of Alberta Press, Edmonton, Alberta, Canada.

Lautze, N. C., and B. F. Houghton (2005), Physical mingling of magma and complex eruption dynamics in the shallow conduit at Stromboli Volcano, Italy, *Geology*, *33*(5), 425–428.

Longo, A., D. Barbato, P. Papale, G. Saccorotti, and M. Barsanti (2008), Numerical simulation of the dynamics of fluid oscillations in a gravitationally unstable, compositionally stratified fissure, *Geol. Soc. London, Spec. Publ.*, *307*(1), 33–44.

Martini, F., C. J. Bean, G. Saccorotti, F. Viveiros, and N. Wallenstein (2009), Seasonal cycles of seismic velocity variations detected using coda wave interferometry at Fogo Volcano, Sao Miguel, Azores, during 2003–2004, *J. Volcanol. Geotherm. Res.*, *181*(3), 231–246.

Nolesini, T., F. Di Traglia, C. Del Ventisette, S. Moretti, and N. Casagli (2013), Deformations and slope instability on Stromboli Volcano: Integration of GBInSAR data and analogue modeling, *Geomorphology*, *180–181*, 242–254.

Parfitt, E. A. (2004), A discussion of the mechanisms of explosive basaltic eruptions, *J. Volcanol. Geotherm. Res.*, *134*(1), 77–107.

Ripepe, M., and E. Gordeev (1999), Gas bubble dynamics model for shallow volcanic tremor at Stromboli, *J. Geophys. Res.*, *104*(B5), 10,639–10,654.

Rivalta, E., K. Pascal, J. Phillips, and A. Bonaccorso (2013), Explosive expansion of a slowly decompressed magma: Evidence for delayed bubble nucleation, *Geochem. Geophys. Geosyst.*, *14*, 3067–3084, doi:10.1002/ggge.20183.

Rosi, M., M. Pistolesi, A. Bertagnini, P. Landi, M. Pompilio, and A. Di Roberto (2013), Stromboli Volcano, Aeolian Islands (Italy): Present eruptive activity and hazards, *Geol. Soc. London Mem.*, *37*(1), 473–490.

Saccorotti, G., B. A. Chouet, M. Martini, and R. Scarpa (1998), Bayesian statistics applied to the location of the source of explosions at Stromboli Volcano, Italy, *Bull. Seismol. Soc. Am.*, *88*, 1099–1111.

Saccorotti, G., and E. Del Pezzo (2000), A probabilistic approach to the inversion of data from a seismic array and its application to volcanic signals, *Geophys. J. Int.*, *143*(1), 249–261.

Taddeucci, J., D. M. Palladino, G. Sottili, D. Bernini, D. Andronico, and A. Cristaldi (2013), Linked frequency and intensity of persistent volcanic activity at Stromboli (Italy), *Geophys. Res. Lett.*, *40*, 3384–3388, doi:10.1002/grl.50652.

Witham, F. (2011), Conduit convection, magma mixing, and melt inclusion trends at persistently degassing volcanoes, *Earth Planet. Sci. Lett.*, *301*(1), 345–352.